Impaired immune cell cytotoxicity in severe COVID-19 is IL-6 dependent

Impaired immune cell cytotoxicity in severe COVID-19 is IL-6 dependent

Alessio Mazzoni[1#], Lorenzo Salvati[1#], Laura Maggi[1], Manuela Capone[1], Anna Vanni[1], Michele Spinicci[1,2], Jessica Mencarini[1,2], Roberto Caporale[3], Benedetta Peruzzi[3], Alberto Antonelli[1], Michele Trotta[2], Lorenzo Zammarchi[1,2], Luca Ciani[1], Leonardo Gori[1], Chiara Lazzeri[4], Andrea Matucci[5], Alessandra Vultaggio[5], Oliviero Rossi[5], Fabio Almerigogna[1,5], Paola Parronchi[1,6], Paolo Fontanari[7], Federico Lavorini[1,8], Adriano Peris[4], Gian Maria Rossolini[1,9], Alessandro Bartoloni[1,2], Sergio Romagnani[1], Francesco Liotta[1,6], Francesco Annunziato[1,3,^,*], Lorenzo Cosmi[1,6,^].

Affiliations

1. Department of Experimental and Clinical Medicine, University of Florence, Florence, Italy
2. Infectious and Tropical Diseases Unit, Careggi University Hospital, Florence, Italy
3. Flow Cytometry Diagnostic Center and Immunotherapy (CDCI), Careggi University Hospital, Florence, Italy
4. Intensive Care Unit and Regional ECMO Referral Centre, Careggi University Hospital, Florence, Italy
5. Immunoallergology Unit, Careggi University Hospital, Florence, Italy
6. Immunology and Cell Therapy Unit, Careggi University Hospital, Florence, Italy
7. Cardiac Anesthesia and Intensive Care Unit, Careggi University Hospital, Florence, Italy
8. Pneumology and Intensive Care Unit, Careggi University Hospital, Florence, Italy
9. Microbiology and Virology Unit, Careggi University Hospital, Florence, Italy

#Contributed equally
^Contributed equally
*Corresponding author

Corresponding Author:

Prof. Francesco Annunziato,
Viale Pieraccini 6, 50139, Florence, Italy
+39 0552758337
francesco.annunziato@unifi.it

Conflict of interest statement: The authors have declared that no conflict of interest exists.

ABSTRACT

Background: Coronavirus disease 19 (COVID-19) is an emerging infectious disease caused by SARS-CoV-2. Anti-viral immune response is crucial to achieve pathogen clearance, however in some patients an excessive and aberrant host immune response can lead to an acute respiratory distress syndrome. The comprehension of the mechanisms that regulate pathogen elimination, immunity, and pathology is essential to better characterize disease progression and widen the spectrum of therapeutic options.

Methods: We performed a flow cytometric characterization of immune cells subsets from 30 COVID-19 patients and correlated these data with clinical outcomes.

Results: COVID-19 patients showed decreased numbers of circulating T, B and NK cells, and exhibited a skewing of CD8+ T cells towards a terminally differentiated/senescent phenotype. In agreement, T CD4+, T CD8+ but also NK cells displayed reduced anti-viral cytokine production capability. Moreover, a reduced cytotoxic potential was identified in COVID-19 patients, particularly in those that required intensive care. The latter group of patients showed also increased serum IL-6 levels, that correlated to the frequency of granzyme-expressing NK cells. Off-label treatment with tocilizumab restored the cytotoxic potential of NK cells.

Conclusion: In conclusion, the association between IL-6 serum levels and the impairment of cytotoxic activity suggests the possibility that targeting this cytokine may restore anti-viral mechanisms.

Funding: This study was supported by funds of Dept. of Experimental and Clinical Medicine of University of Florence (ex-60%) derived from Ministero dell'Istruzione, dell'Università e della Ricerca (Italy).

INTRODUCTION

SARS-CoV-2 is the etiologic agent of coronavirus disease 19 (COVID-19) and belongs to the same group of ribonucleic acid (RNA) viruses that caused severe acute respiratory syndrome (SARS) and Middle East respiratory syndrome (MERS) in the past (1,2,3). At the time of this publication the World Health Organization (WHO) has considered COVID-19 as a new pandemic disease (4). As of April 27, 2020, there have been 2,878,196 confirmed COVID-19 cases globally; in Italy, 197,675 confirmed cases have been reported with a total of 26,644 deaths (5). Coronaviruses are enveloped, non-segmented, single-stranded, positive-sense RNA viruses named after the observation on electron microscopy of their corona- or crown-like surface projections, that correspond to large surface spike proteins. Coronaviruses are classified in the Nidovirales order (6). These viruses are host specific and can infect humans and a variety of different animals as well. The previously unknown coronavirus, named SARS-CoV-2, was discovered in December 2019 in Wuhan, in the province of Hubei, China and was sequenced and isolated by January 2020 (7-9). SARS-CoV, MERS-CoV and SARS-CoV-2 are all in the genus betacoronavirus (6). SARS-CoV-2 infection clinically presents with fever, nonproductive cough, and respiratory distress that tends to be more common in adults than in children (10). Coronavirus entry into host cells is mediated by the transmembrane spike (S) glycoprotein that forms homotrimers protruding from the viral surface (11). SARS-CoV and several SARS-related coronaviruses interact directly with angiotensin-converting enzyme 2 (ACE2) via S protein to enter target cells (12, 13). It has been recently shown that ACE2 could also mediate SARS-CoV-2 S-dependent entry into cells, thus representing a functional receptor for this newly emerged coronavirus (14). ACE2 is expressed in the respiratory tract, by mucosal epithelial cells, lung alveolar type 2 pneumocytes, arterial and venous endothelial cells but also in other tissues, including the gastrointestinal tract, accounting for the mild enteritis that sometimes is present in COVID-19 patients (15, 16).

Both innate and adaptive immune responses are critical for the control of viral infections. Natural killer (NK) cells exert the primary control during acute viral infection, but cytotoxic CD8+ T lymphocytes (CTLs) are critical for long-term surveillance (17-20). The antiviral effects of NK and CD8+ T cells can be mediated by direct cytotoxicity or through the release of IFN-γ. IFN-γ is able to directly interfere with viral replication, as well as to indirectly affect viral clearance through the activation of Type 1 T helper (Th1)-mediated responses and through MHC class I pathway enhancement (21). Antiviral cytotoxic responses are mediated principally by perforin and granzymes. Recovery from viral infections requires the generation of effective antiviral responses that can eliminate, or at least control, the infecting pathogen. Severe viral infections may induce per se immunopathology, however dysregulated antiviral immune responses can contribute to tissue damage. Thus, it is important to understand the mechanisms regulating pathogen elimination, immunity, and pathology to prevent immune-mediated damage (22, 23). In trying to treat common infections, it is important to understand the mechanisms that regulate pathogen elimination, immunity, and pathology, so that immune-mediated damage is prevented. The aim of the present study was to perform a deep immunophenotyping of peripheral blood mononuclear cells (PBMNC) from patients affected by COVID-19 and to correlate these data with clinical parameters and outcomes.

RESULTS

Clinical evaluation of COVID-19 patients.

We evaluated 30 patients affected by COVID-19 that were admitted to Careggi University Hospital. SARS-CoV-2 infection was confirmed by positive RT-PCR on nasopharyngeal swab in accordance with WHO interim guidances (24). All specimens were re-tested and deemed positive for SARS-CoV-2 by the Italian National Institute of Health. The clinical characteristics of the 30 patients are shown in Table S1. The median age of the patients was 70 years (range 36-85 years), the mean age was 65.9 years. 60% of the cases were male. The mean age was 67.9 years for men and 63 years for women. On the day of the immunologic analysis, which was performed on average 9.2 days after the onset of the disease and 3.5 days after the hospital admission, the most common symptoms were fever (53%) and cough (40%), while diarrhoea was an uncommon manifestation (3%). All patients presented with chest imaging abnormalities (Table S1); the most frequent radiologic findings were pulmonary consolidations (40%) and multiple bilateral patchy opacities (30%), compatible with interstitial pneumonia. Table S2 reports laboratory results on the day of immunologic analysis. Lymphocytopenia (median 830 cells/μl) was present in 93% of the patients with a median neutrophil-lymphocyte ratio of 7.3 and eosinopenia (median 20 cells/μl) in 52% of subjects. Almost all patients had elevation of acute-phase proteins: C-reactive protein (CRP, median 60.5 mg/L), fibrinogen (median 510 mg/dL) and ferritin (median 795 ng/mL). D-dimer (median 940 ng/mL) and lactate dehydrogenase (median 271 U/L) were also increased. A majority of the patients (80%) had at least one comorbidity and hypertension was present in 50% of the cases (Table S1). Two women were pregnant at 25 weeks of gestation. On the day of analysis, patients were receiving antiviral treatment (83%), hydroxychloroquine (80%), and intravenous antibiotics (53%) (Table S1). Oxygen therapy was being administered in 77% of the patients; the mean PaO_2/FiO_2 ratio was 261 (median, 268) (Table S3). Acute respiratory distress syndrome (ARDS) during the course of COVID-19 occurred in 14 cases (53%). Among the 30

hospitalized patients considered in this study, 12 (40%) were admitted to the intensive care unit (ICU). ICU patients had more severe pulmonary involvement than patients not admitted to the ICU (mean PaO_2/FiO_2 ratio 171 vs 314, mean SaO_2/FiO_2 ratio 170 vs 372, mean Alveolar-arterial O_2 gradient 326 vs 72 mmHg, respectively) ($p<0.001$). In addition, they presented higher neutrophil and lower lymphocyte counts ($p<0.05$), higher neutrophil-lymphocyte ratio ($p<0.01$), higher lactate dehydrogenase ($p<0.001$), as well as higher CRP ($p<0.05$) and IL-6 ($p<0.01$) compared to the non-ICU patients.

COVID-19 patients are characterized by lymphopenia.

In order to provide direct evaluation of leukocytes homeostasis, we studied the immunological characteristics of peripheral blood leukocytes derived from SARS-CoV-2 infected patients. As shown in Figure 1A, COVID-19 patients were characterized by a significant increase of neutrophils and a significant decrease of lymphocytes, eosinophils and basophils absolute numbers in the peripheral blood as compared to age and sex matched healthy subjects. Total leukocytes as well as monocytes absolute numbers were comparable between COVID-19 patients and healthy subjects (Figure 1A). In order to better understand which lymphocyte population was affected, we performed a flow cytometric analysis of circulating leukocytes. As shown in Figure 1B, T (CD3+), B (CD3-CD19+) and NK (CD3-CD56+) cells absolute numbers were significantly reduced in COVID-19 patients when compared to healthy subjects. In addition, among CD3+ cells, we found a significant reduction of CD4+, CD8+ and CD56+ (NKT) cells (Figure 1C). More importantly, we found that CD4+/CD8+ T cell ratio in COVID-19 patients was significantly higher than in healthy subjects (Figure 1D). The frequencies of TCR alpha/beta and gamma/delta-positive T lymphocytes showed no significant differences in COVID-19 patients compared to healthy subjects, as well as the frequencies of Treg and Tfh cells (data not shown).

CD3+CD8+ lymphocytes from COVID-19 patients have a senescent phenotype.

Since all lymphocyte populations were significantly reduced in COVID-19 patients, we evaluated, in the context of B and T lymphocytes, whether the frequencies of the different subpopulations at different stages of maturation had varied.

As shown in Figure S1 (A-E), while the frequency of naïve (IgD+CD27-), memory not switched (IgD+CD27+), memory switched (IgD-CD27+) B lymphocytes and plasmablasts ($CD27^{high}CD38^{high}$) were not significantly affected, the frequency of transitional ($IgM^{high}CD38^{high}$) B lymphocytes was significantly reduced ($p<0.001$) in COVID-19 patients when compared to reference ranges (25).

In the context of CD4+ T lymphocytes, we found a significant increase of the frequency of T central memory (Tcm, CD45RA-CCR7+) cells, whereas naïve (CD45RA+CCR7+), T effector memory (Tem, CD45RA-CCR7-), T effector memory CD45RA+ (TEMRA, CD45RA+CCR7-) and HLA-DR+ cells from COVID-19 patients did not show different values when compared to healthy subjects (Figure 2A and Figure S2). Since total count of CD4+ T cells is significantly lower in COVID-19 patients than in healthy subjects this finding means that, among CD4+ T cells, the naïve, Tem, and TEMRA subsets are mostly impaired in these patients, whereas Tcm are relatively conserved.

More importantly, flow cytometric analysis of CD8+ T lymphocytes revealed statistically significant reduction of naïve (CD45RA+CCR7+) and Tcm (CD45RA-CCR7+) in COVID-19 patients when compared to healthy subjects (Figure 2B and Figure S2). On the other side, frequencies of TEMRA (CD45RA+CCR7-) and senescent (CD57+) CD8+ T cells were significantly higher in COVID-19 patients when compared to healthy subjects (Figure 2B and Figure S2). Tem (CD45RA-CCR7-) and HLA-DR+ CD8+ T cells from COVID-19 patients did not show relevant variations when compared to healthy subjects (Figure 2B and Figure S2). These findings suggest that CD8+ T cells in COVID-19 patients are skewed towards a terminally differentiated and senescent phenotype.

Lymphocytes from COVID-19 patients are characterized by significant reduction of type 1 cytokines and cytotoxic potential.

After evaluating the different lymphocyte subpopulations in terms of differentiation stages, we stimulated peripheral blood cells with PMA and ionomycin in order to evaluate their ability to produce cytokines (Figure S3). In particular, we focused on the cytokines described being highly protective against viral infections, i.e. the IFN-γ, TNF-α and IL-2. As shown in Figure 3A, COVID-19 patients showed a significantly increased frequency of IL-2-producing CD4+ T cells, while CD8+ T lymphocytes of the same patients showed a significantly reduced frequency of IL-2 when compared with healthy subjects.

COVID-19 patients showed a significantly reduced frequency of IFN-γ-producing CD4+ and CD8+ T cells when compared to healthy subjects (Figure 3B). No differences were found in NK cells (Figure 3B) in terms of IFN-γ production. Furthermore, COVID-19 patients showed a significantly reduced frequency of TNF-α-producing NK cells when compared with healthy subjects (Figure 3C). It should be noted that the CD4+ and CD8+ T lymphocytes also showed a reduced ability to produce TNF-α even if these data did not reach statistical significance (Figure 3C). Since it has been previously shown that CD4+ and CD8+ lymphocytes able to produce more than one cytokines (polyfunctional T cells) are most protective against viral infections (26), we simultaneously evaluated IL-2, IFN-γ and TNF-α expression on a cohort of COVID-19 patients, as well as healthy controls (Figure S4A). As shown in Figure S4B-C, while no differences were detected in CD4+ T cells between COVID-19 and healthy subjects, significantly reduced frequencies of IL-2+IFN-γ+TNF-α+ and IL-2+IFN-γ+TNF-α- CD8+ T cells within COVID-19 patients were detected.

Since the antiviral effects of lymphocytes can be exerted also by direct cytotoxicity mediated principally by perforin and granzymes, we evaluated the cytoplasmic expression of these two molecules in CD4+, CD8+ T lymphocytes and NK cells, to define their cytotoxic potential

(Figure S5). As shown in Figure 3D-E, NK cells from COVID-19 patients showed significantly reduced percentages of both perforin and granzyme A as compared to healthy donors. While CD3+CD4+ T cells from COVID-19 patients showed significantly reduced frequencies of granzyme A, no differences were appreciable regarding the frequency of perforin positive cells in this cell subset and of both perforin and granzyme A in CD3+CD8+ T cell population (Figure 3D-E).

COVID-19 patients admitted to the ICU show significantly reduced NK cell numbers and cytotoxic potential.

A significant fraction of patients with COVID-19 develops ARDS and needs hospitalization in ICU, requiring invasive mechanical ventilation (27). We therefore investigated if there was a significant variation of the previously identified immune parameters between patients who were admitted to the ICU (ICU patients) and those not admitted to the ICU (non-ICU patients) during the course of the hospitalization.

As shown in Figure 4A, ICU patients were characterized by a significant increase of neutrophils and a significant decrease of lymphocytes absolute numbers in the peripheral blood as compared to non-ICU patients. Total leukocytes as well as monocytes, eosinophils and basophils absolute numbers were comparable between the two group of patients (Figure 4A). As shown in Figure 4B, flow cytometric analysis of circulating leukocytes revealed that T (CD3+), and NK (CD3-CD56+), but not B (CD19+), cells absolute numbers were significantly reduced in ICU when compared to non-ICU patients. In addition, among CD3+ cells, we found a significant reduction of CD4+, but not CD8+ and CD56+ (NKT) cells in ICU when compared to non-ICU patients (Figure 4C). In the context of CD4+ T lymphocytes we found no significant differences of the frequency of naïve (CD45RA+CCR7+), Tcm (CD45RA-CCR7+), Tem (CD45RA-CCR7-), TEMRA (CD45RA+CCR7-) and HLA-DR+ cells between the two groups of patients (Figure 4D).

On the other side, flow cytometric analysis of CD8+ T lymphocytes revealed statistically significant reduction of Tem (CD45RA-CCR7-) and increase of TEMRA (CD45RA+CCR7) cells in ICU when compared to non-ICU patients (Figure 4E). As shown in Figure 4E, naïve (CD45RA+CCR7+), Tcm (CD45RA-CCR7+), senescent (CD57+) and HLA-DR+ CD8+ T cells did not differ between the two groups of patients (Figure 4E).

As shown in Figure 5A-C, no differences were identified between the two groups of patients regarding the frequencies of CD3+CD4+, CD3+CD8+ and NK cells producing IFN-γ, TNF-α, and IL-2. Regarding T cell polyfunctionality, our analysis performed on a cohort of ICU and non-ICU patients showed no statistically significant differences between the two groups (Figure S6).

Finally, the frequencies of both perforin and granzyme A were reduced in NK cells from ICU patients, with statistical significance only for granzyme A (Figure 5D-E). All together, these data support the concept that in ICU patients the depletion of CD3+CD4+ T cells becomes even more pronounced, as well as the accumulation of terminally differentiated CD3+CD8+ T cells and NK cells with reduced cytolitic potential, leading to altered immunological protection.

High IL-6 serum levels in ICU patients inversely correlate with NK cytotoxic potential, that can be restored by tocilizumab treatment.

Since SARS-CoV-2 infection has been reported to associate with increased IL-6 serum levels (28), we evaluated this pro-inflammatory cytokine in the sera of ICU and non-ICU patients. As shown in Figure 6A, IL-6 serum levels were significantly higher in ICU as compared to non-ICU patients. More importantly, among those cellular parameters that we found significantly altered in ICU versus non-ICU patients, we observed a significant inverse correlation only between the serum levels of IL-6 and the frequency of NK cells expressing granzyme A (Figure 6B).

Since higher serum IL-6 levels correlated with lower granzyme A expression on NK cells, we investigated if blocking IL-6 axis in COVID-19 patients with tocilizumab could restore granzyme A expression. For this reason, we recruited 5 ICU patients candidated to tocilizumab treatment, characterized by high IL-6 serum levels and low frequency of NK cells expressing granzyme A. Tocilizumab treatment led to a reduction of CRP levels, suggesting that efficacious neutralization of IL-6 activity was achieved (Figure 6C). As shown in Figure 6D, an increased lymphocyte count was observed after tocilizumab treatment. From a functional point of view, no significant increase was observed in the frequencies of CD8+ T cells expressing granzyme A or perforin (Figure 6 E and Figure F). However, treatment with tocilizumab significantly increased the expression of granzyme A and perforin on NK cells (Figure 6 G and Figure H), and induced a mild amelioration of PaO_2/FiO_2 ratio in four out of five patients (Figure 6I).

DISCUSSION

Cytotoxic lymphocytes such as CD8+ T lymphocytes and NK cells are necessary for the control of viral infections (17-20), and the functional exhaustion of these cells is correlated with disease progression (29, 30). On the other side, exaggerated or not controlled immune responses can be responsible for the organ damage that sometimes accompanies the infection (16,21). Aim of our work was to perform a phenotypic and functional characterization of the immune response in SARS-CoV-2 infected patients hospitalized at the Careggi University Hospital, Florence, Italy.

We enrolled 30 patients, whose main clinical features are reported in Table 1. The first clear data emerging from our analysis was the reduction of circulating lymphocytes compared to a cohort of healthy subjects, as already reported (27). Circulating basophils and eosinophils were also significantly lower in COVID-19 patients, while neutrophils were higher in patients than in controls. Thus, no differences were observed in the total number of WBC. By investigating which population of lymphocytes was mainly affected, we found that all subsets, namely T, B, and NK cells were reduced. Among CD3+ T cells, we found a reduction in both CD4+ and CD8+ subsets, but also in the CD56+ fraction, namely the NKT subset. Interestingly, the reduction of T cells number was more pronounced in the CD8+ cytotoxic cells than in CD4+ T helper subset. Despite the reduction of total absolute numbers of B cells in COVID-19 patients, only transitional B cells exhibited significant lower levels than reference ranges. This finding, together with a deep characterization of B cell functions, will require additional investigations in the next future. The picture was quite different when T cells, in particular the CD8+ subset, were analysed. Indeed, we found a significant increase of TEMRA and CD57+CD8+ cells with a parallel decrease of the naïve subset, indicating a significant enrichment of senescent cytotoxic CD8+ T cells. These data are in agreement with previous studies performed on acute and chronic viral infections showing that during these conditions CD8+ T cells acquire an exhausted senescent phenotype (31, 32). Accordingly, when we

analysed the ability of CD4+ and CD8+ T lymphocytes and NK cells to produce cytokines following polyclonal stimulation in vitro, we found in COVID-19 patients reduced frequencies of IFN-γ producing cells in both CD4+ and CD8+ T cells, as well as lower frequencies of TNF-α producing cells among NK cells. Interestingly, COVID-19 patients showed a significant reduction of CD8+ polyfunctional cell subsets which have been described to be highly protective in viral infected patients (26). These findings demonstrated that COVID-19 patients not only exhibit lower numbers of lymphocytes, but also a decreased capacity to produce TNF-α and IFN-γ, two cytokines that play an important role in the clearance of intracellular pathogens (33).

To further explore the capacity of the immune system to clear the infection, we next moved to the evaluation of the cytolytic potential of each lymphocyte subset, and we found that in COVID-19 patients intracellular expression of granzyme by circulating NK was significantly lower than in healthy controls. Perforin showed the same trend, even if not statistically significant. Collectively, these data demonstrated that COVID-19 patients have a functionally impaired anti-viral response.

In order to try to correlate this impairment with disease activity, we divided our cohort of patients in two groups, non-ICU (patients that didn't need intensive care), and ICU (patients admitted to the intensive care unit), searching for differences in terms of immunological functions and/or serological markers of disease activity. Interestingly, when the cytolytic potential was assessed, we found lower frequencies of granzyme A expressing NK cells in the ICU group respect to the non-ICU group. In addition, the ICU patients showed lower numbers of circulating CD3+CD4+ and NK lymphocytes and higher levels of serum IL-6. Moreover, serum IL-6 levels inversely correlated with the frequency of granzyme-expressing NK cells. The observation that serum IL-6 levels correlates with the impairment of cytotoxic activity in COVID-19 patients is in agreement with some reports in literature demonstrating that, both in

murine and in human settings, the exposure to high levels of IL-6 inhibits NK cell cytotoxicity and down-regulates the expression of perforin and granzyme (34, 35, 36, 37).

IL-6 is a pleiotropic proinflammatory multifunctional cytokine produced by a variety of cell types, whose serum levels are elevated in various inflammatory and autoimmune disorders such as rheumatic diseases and cytokine release syndrome (38). The possibility to use an anti-IL-6 receptor (IL-6R) monoclonal antibody in COVID-19 patients is emerging as a potential therapeutic option, and is currently under evaluation in chinese and italian clinical trials (39, 40).

Starting from this background, we took the opportunity to evaluate five COVID-19 ICU patients that underwent off-label treatment with tocilizumab. These patients were evaluated before and after (72 hours) tocilizumab treatment. All patients treated with tocilizumab displayed an increased expression of both perforin and granzyme in NK cells and a parallel decrease of CRP, which is considered as a marker of IL-6 mediated inflammation. Four out of five patients also showed a mild increase of the PaO_2/FiO_2 ratio, even if this observation is not sufficient to sustain that tocilizumab has clinical efficacy. Our data are in agreement with studies showing that exuberant inflammatory responses caused by pathogenic human coronaviruses reduce T cell responses (41). Regarding SARS-CoV infection, this event occurs via a TNF-mediated T cell apoptosis, thus resulting in uncontrolled inflammatory responses (42). Indeed, it has been demonstrated that CoV-specific T cells are crucial not only for virus clearance but also for limiting further damage to the host, dampening overactive innate immune responses (43, 44, 45). On the other hand, the clearance of the infective agent coincides with the elimination of the trigger that maintains the pathologic hyper-inflammation.

Our work pointed out some immunological features of COVID-19 patients and focused on cytotoxic lymphocytes as the subsets mostly impaired. It is important to underline that we enrolled patients that required hospitalization during the course of their disease and some of them were treated with antiviral agents or even required intensive care. Thus, it is possible that

some of the findings highlighted in this work represent a “core” immunological signature that develops at late stages of severe infections. The inverse correlation between serum levels of IL-6 and the impairment of cytotoxic activity, suggests the possibility that this cytokine may be responsible for the impairment of cytotoxic lymphocytes, directly or indirectly. This hypothesis is further strengthened by the recovery of perforin and granzyme expression in NK cells after IL-6R treatment. In this view, the therapeutic blocking of IL-6 axis should be considered not only as a mechanism to suppress noxious systemic inflammation but also to restore the protective anti-viral potential.

In conclusion, the present work suggests that targeting inflammation is a promising tool for the treatment of COVID-19, and provides evidence on the biological mechanism by which tocilizumab can contribute to the clearance of SARS-CoV-2 infection.

METHODS

Patients

30 SARS-CoV-2 infected patients were recruited at the Careggi University Hospital (Azienda Ospedaliero-Universitaria Careggi), Florence, Italy by the Infective and Tropical Diseases Unit and the Intensive Care Unit. SARS-CoV-2 infection was confirmed by routine diagnostic PCR amplification of viral genes from nasopharyngeal swabs. 30 blood donors were recruited as healthy controls. The median age of healthy controls was 63.5 years, the mean age 64.2 years, 50% of the cases were males (Table S4). All patients and controls were of Caucasian origin. For longitudinal study, peripheral blood samples were collected prior and after 72 hours post tocilizumab treatment. Tocilizumab dosage was 8 mg/Kg of body weight, followed by 8 mg/Kg after 12 hours.

Immunophenotyping by flow cytometry

For the analysis of lymphocyte cell subsets by surface markers expression, an aliquot (600 µl) of blood specimens was incubated with ammonium chloride for 5 minutes at RT to lyse red blood cells. Following two washes in PBS+BSA 0,5%, the resulting white blood cells (WBC) were stained for 15 minutes with fluorochrome-conjugated monoclonal antibodies (mAbs). List of all fluorochrome-conjugated mAbs is reported in Table S5. Samples were acquired on a BD LSR II flow cytometer (BD Biosciences). All flow cytometric analysis were performed following published guidelines (46).

Evaluation of cytokine production by flow cytometry.

PBMNC were obtained following density gradient centrifugation of blood samples. PBMNC were then polyclonally stimulated for 5 hours with PMA (10ng/mL) and ionomycin (1µM), the last 3 in presence of brefeldin A (5µg/mL). Cells were then fixed in formaldehyde 2% for 15 minutes at RT, washed in PBS+BSA 0,5% and then stained intracellular with fluorochrome-

conjugated mAbs in presence of the permeabilizing agent saponin (0,5%). List of all fluorochrome-conjugated antibodies used is reported in Table S5. Samples were acquired on a BD LSR II flow cytometer (BD Biosciences).

Evaluation of cytotoxic molecules by flow cytometry.

PBMNC were directly fixed and stained intracellular as previously described using fluorochrome-conjugated mAbs (Table S5). Samples were acquired on a BD LSR II flow cytometer (BD Biosciences).

Serum cytokine detection.

Dosages of serum IL-6 was performed using an IL-6 human instant ELISA kit (Invitrogen) on an automated DSX instrument (DYNEX Technologies).

Statistics

Unpaired 2-tailed Student's t-test was used for comparison of clinical and laboratory findings, and for flow cytometric analysis of healthy controls versus COVID-19 patients. p values ≤ 0.05 were considered significant. Pearson's correlation coefficients were used to calculate the correlations.

Study approval

The procedures followed in the study were approved by the Careggi University Hospital Ethical Committee (protocol 16859). Written informed consent was obtained from recruited patients.

AUTHOR CONTRIBUTIONS

Fr.L., Fr.A., Lo.C., A.B. designed research studies. Al.M., L.S., L.M., M.C., An.V., A.A. R.C., B.P., An.M., Al.V. conducted experiments; Al.M., L.S., L.M., M.C., M.S., J.M., L.Z., Fr.L., F.A., Lo.C. acquired data; Al.M., L.S., L.M., M.C., Fr.L., F.A., Lo.C. analyzed data;

M.S., J.M., M.T., L.Z., L.G., Lu.C., C.L., P.F., Fe.L., A.P., A.B. collected peripheral blood samples and acquired informed consent; Fr.A., L.C., Fr.L., Al.M., L.S., L.M. wrote the manuscript; S.R., Fa.A., P.P., G.M.R., O.R. provided advice. All authors revised the manuscript and gave final approval for publication.

REFERENCES

1. Drosten C, et al. Identification of a Novel Coronavirus in Patients With Severe Acute Respiratory Syndrome. *N Engl J Med.* 2003;348(20):1967–1976.

2. Ksiazek TG, et al. SARS Working Group. A Novel Coronavirus Associated With Severe Acute Respiratory Syndrome. *N Engl J Med*. 2003:15;348(20):1953–1966.

3. Zaki AM, et al. Isolation of a Novel Coronavirus From a Man With Pneumonia in Saudi Arabia. *N Engl J Med*. 2012;367(19):1814–1820.

4. World Health Organization. World Health Organization Website. WHO Director - General's opening remarks at the media briefing on COVID-19. 11th March 2020. https://www.who.int/dg/speeches/detail/who-director-general-s-opening-remarks-at-the-media-briefing-on-covid-19---11-march-2020. Accessed March, 25 2020.

5. World Health Organization. World Health Organization Website. Coronavirus disease 2019 (COVID-19) Situation Report – 98. 27th April 2020. https://www.who.int/emergencies/diseases/novel-coronavirus-2019/situation-reports. Accessed April, 28 2020.

6. Gorbalenya AE, et al. The species Severe acute respiratory syndrome-related coronavirus: classifying 2019-nCoV and naming it SARS-CoV-2. *Nat Microbiol*. 2020;5:536–544.

7. Huang C, et al. Clinical features of patients infected with 2019 novel coronavirus in Wuhan, China. *Lancet.* 2020;395(10223):497–506.

8. Zhou P, et al. A pneumonia outbreak associated with a new coronavirus of probable bat origin. *Nature* 2020;579:270–273.

9. Zhu N, et al. A Novel Coronavirus from Patients with Pneumonia in China, 2019. *N Engl J Med.* 2020;382(8):727–733.

10. Lu X, et al. Chinese Pediatric Novel Coronavirus Study Team. SARS-CoV-2 Infection in Children. *N Engl J Med*. 2020. *N Engl J Med.* 2020;382(17):1663–1665.

11. Tortorici MA, Veesler D. Structural insights into coronavirus entry. *Adv Virus Res.* 2019;105:93–116.

12. Ge XY, et al. Isolation and characterization of a bat SARS-like coronavirus that uses the ACE2 receptor. *Nature*. 2013;503(7477):535–538.

13. Li W, et al. Angiotensin-converting enzyme 2 is a functional receptor for the SARS coronavirus. *Nature*. 2003;426(6965):450–454.

14. Hoffmann M, et al. SARS-CoV-2 Cell Entry Depends on ACE2 and TMPRSS2 and Is Blocked by a Clinically Proven Protease Inhibitor. *Cell.* 2020;181(2):271–280.e8.

15. Hamming I, et al., Tissue distribution of ACE2 protein, the functional receptor for SARS coronavirus. A first step in understanding SARS pathogenesis. *J Pathol*. 2004;203(2):631–637.

16. Wan Y, et al. Receptor Recognition by the Novel Coronavirus from Wuhan: an Analysis Based on Decade-Long Structural Studies of SARS Coronavirus. *J Virol*. 2020;94(7):e00127–20.

17. National Research Project for SARS, Beijing Group. The involvement of natural killer cells in the pathogenesis of severe acute respiratory syndrome. *Am J Clin Pathol*. 2004;121(4):507–511.

18. Chen J, et al. Cellular immune responses to severe acute respiratory syndrome coronavirus (SARS-CoV) infection in senescent BALB/c mice: CD4+ T cells are important in control of SARS-CoV infection. *J Virol.* 2010;84(3):1289–1301.

19. Marquardt N, et al. The Human NK Cell Response to Yellow Fever Virus 17D Is Primarily Governed by NK Cell Differentiation Independently of NK Cell Education. *J. Immunol.* 2015;195(7):3262–3272.

20. Song H, et al. Monkeypox virus infection of rhesus macaques induces massive expansion of natural killer cells but suppresses natural killer cell functions. *PLoS One.* 2013;8(10):e77804.

21. Zhou F. Molecular mechanisms of IFN-gamma to up-regulate MHC class I antigen processing and presentation. *Int Rev Immunol*. 2009;28(3-4):239–260.

22. Duan S, Thomas PG. Balancing Immune Protection and Immune Pathology by CD8(+) T-Cell Responses to Influenza Infection. *Front Immunol*. 2016;7:25.

23. Shin, E., Sung, P., Park, S. Immune responses and immunopathology in acute and chronic viral hepatitis. *Nat Rev Immunol.* 2016:16:509–523.

24. World Health Organization. Laboratory testing for coronavirus disease (COVID-19) in suspected human cases: interim guidance. World Health Organization. March, 19 2020.

25. Boldt A, et al. Eight-color immunophenotyping of T-, B-, and NK-cell subpopulations for characterization of chronic immunodeficiencies. *Cytometry B Clin Cytom.* 2014;86(3):191–206.

26. Harari A et al. Functional signatures of protective antiviral T-cell immunity in human virus infections. *Immunol Rev.* 2006;211:236–254.

27. Guan WJ, et al. China Medical Treatment Expert Group for Covid-19. Clinical Characteristics of Coronavirus Disease 2019 in China. [published online February 28, 2020]. *N Engl J Med*. 2020. doi: 10.1056/NEJMoa2002032

28. Chen G, et al. Clinical and immunological features of severe and moderate coronavirus disease 2019. [published online March 27, 2020]. *J Clin Invest.* 2020. pii: 137244. doi: 10.1172/JCI137244.

29. McLane LM, et al. CD8 T Cell Exhaustion During Chronic Viral Infection and Cancer. *Annu Rev Immunol*. 2019;37:457–495.

30. Bi J, Tian Z. NK Cell Exhaustion. *Front Immunol*. 2017;8:760.

31. Erickson JJ, et al. Acute Viral Respiratory Infection Rapidly Induces a CD8+ T Cell Exhaustion-like Phenotype. *J Immunol.* 2015;195(9):4319–4330.

32. Hashimoto M, et al. CD8 T Cell Exhaustion in Chronic Infection and Cancer: Opportunities for Interventions. *Annu Rev Med.* 2018;69:301–318.

33. Annunziato F, Romagnani C, Romagnani S. The 3 major types of innate and adaptive cell-mediated effector immunity. *J Allergy Clin Immunol*. 2015;135(3):626–635.

34. Tanner J, Tosato G. Impairment of natural killer functions by interleukin 6 increases lymphoblastoid cell tumorigenicity in athymic mice. *J Clin Invest.* 1991;88:239–247.

35.Vredevoe DL, et al. Interleukin-6 (IL-6) expression and natural killer (NK) cell dysfunction and anergy in heart failure. *Am J Cardiol.* 2004;93:1007–1011.

36. Scheid C, et al. Immune function of patients receiving recombinant human interleukin-6 (IL-6) in a phase I clinical study: induction of C-reactive protein and IgE and inhibition of natural killer and lymphokine-activated killer cell activity. *Cancer Immunol Immunother*. 1994;38:119–126.

37. Cifaldi L, et al. Inhibition of natural killer cell cytotoxicity by interleukin-6: implications for the pathogenesis of macrophage activation syndrome. *Arthritis Rheumatol*. 2015;67(11):3037–3046.

38. Shimabukuro-Vornhagen A, et al. Cytokine release syndrome. *J Immunother Cancer*. 2018;6(1):56.

39. A multicenter, randomized controlled trial for the efficacy and safety of tocilizumab in the treatment of new coronavirus pneumonia (COVID-19). Available from: http://www.chictr.org.cn/showprojen.aspx?proj=49409. ChiCTR2000029765. Accessed March, 26 2020.

40. Multicenter study on the efficacy and tolerability of tocilizumab in the treatment of patients with COVID-19 pneumonia. Available from: https://www.clinicaltrialsregister.eu/ctr-search/trial/2020-001110-38/IT. EudraCT number: 2020-001110-38 (TOCIVID-19). Accessed March, 26 2020.

41. Channappanavar R, Perlman S. Pathogenic human coronavirus infections: causes and consequences of cytokine storm and immunopathology. *Semin Immunopathol.* 2017;39:529–539.

42. Channappanavar R, et al. T cell-mediated immune response to respiratory coronaviruses. *Immunol Res.* 2014;59(1-3):118–128.

43. Kim KD, et al. Adaptive immune cells temper initial innate responses. *Nat Med.* 2007;13(10):1248–1252.

44. Palm NW, Medzhitov R. Not so fast: adaptive suppression of innate immunity. *Nat Med.* 2007;13(10):1142–1144

45. Zhao J, et al. T cell responses are required for protection from clinical disease and for virus clearance in severe acute respiratory syndrome coronavirus-infected mice. *J Virol.* 2010;84(18):9318–9325.

46. Cossarizza A, et al. Guidelines for the use of flow cytometry and cell sorting in immunological studies (second edition). Eur J Immunol. 2019;49(10):1457-1973.

Figures and figure legends

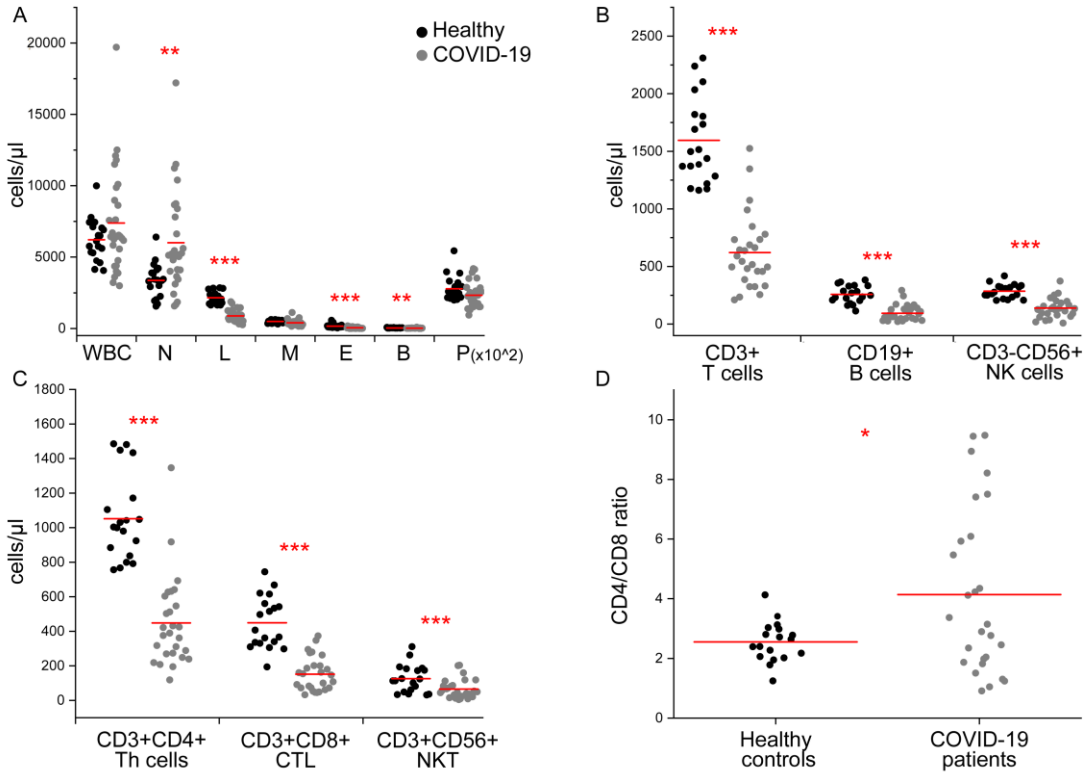

Figure 1. Absolute numbers of circulating white blood cells in COVID-19 patients

(A) Absolute numbers of total white blood cells (WBC), neutrophils (N), lymphocytes (L), monocytes (M), eosinophils (E), basophils (B), platelets (P) in healthy controls (black dots) and COVID-19 patients (gray dots). (B) Absolute numbers of CD3+ T cells, CD19+ B cells and CD56+ NK cells in healthy controls (black dots) and COVID-19 patients (gray dots). (C) Absolute numbers of CD3+CD4+ T helper cells, CD3+CD8+ cytotoxic T cells (CTL), CD3+CD56+ NKT cells in healthy controls (black dots) and COVID-19 patients (gray dots). (D) Ratio of CD4/CD8 absolute numbers cells in healthy controls (black dots) and COVID-19 patients (gray dots). Red lines represent mean values for each population. Data have been obtained from 19 healthy controls and 27 COVID-19 patients. *p<0.05; **p<0.01; ***p<0.001 calculated with Student's T test.

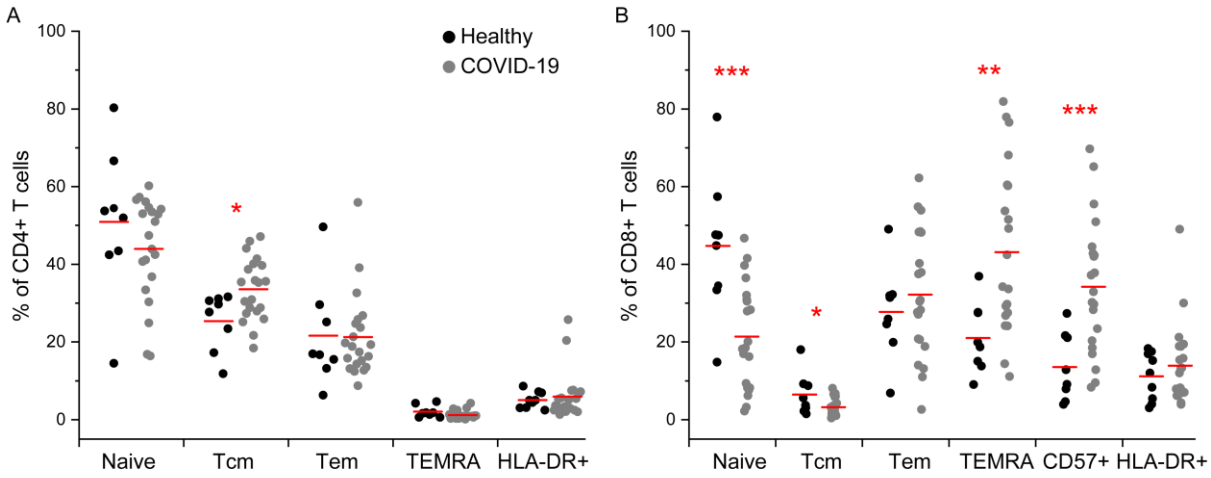

Figure 2. Frequency of CD4+ and CD8+ T cell subsets in COVID-19 patients

(A) Frequency of naïve (CD45RA+CCR7+), central memory (CD45RA-CCR7+), effector memory (CD45RA-CCR7-), TEMRA (CD45RA+CCR7-) and HLA-DR+ cells among CD4+ T cells in healthy controls (black dots) and COVID-19 patients (gray dots). (B) Frequency of naïve (CD45RA+CCR7+), central memory (CD45RA-CCR7+), effector memory (CD45RA-CCR7-), TEMRA (CD45RA+CCR7-), senescent (CD57+) and HLA-DR+ cells among CD8+ T cells in healthy controls (black dots) and COVID-19 patients (gray dots). Red lines represent mean values for each population. Data have been obtained from 8 healthy controls and 21 COVID-19 patients. *p<0.05; **p<0.01; ***p<0.001 calculated with Student's T test.

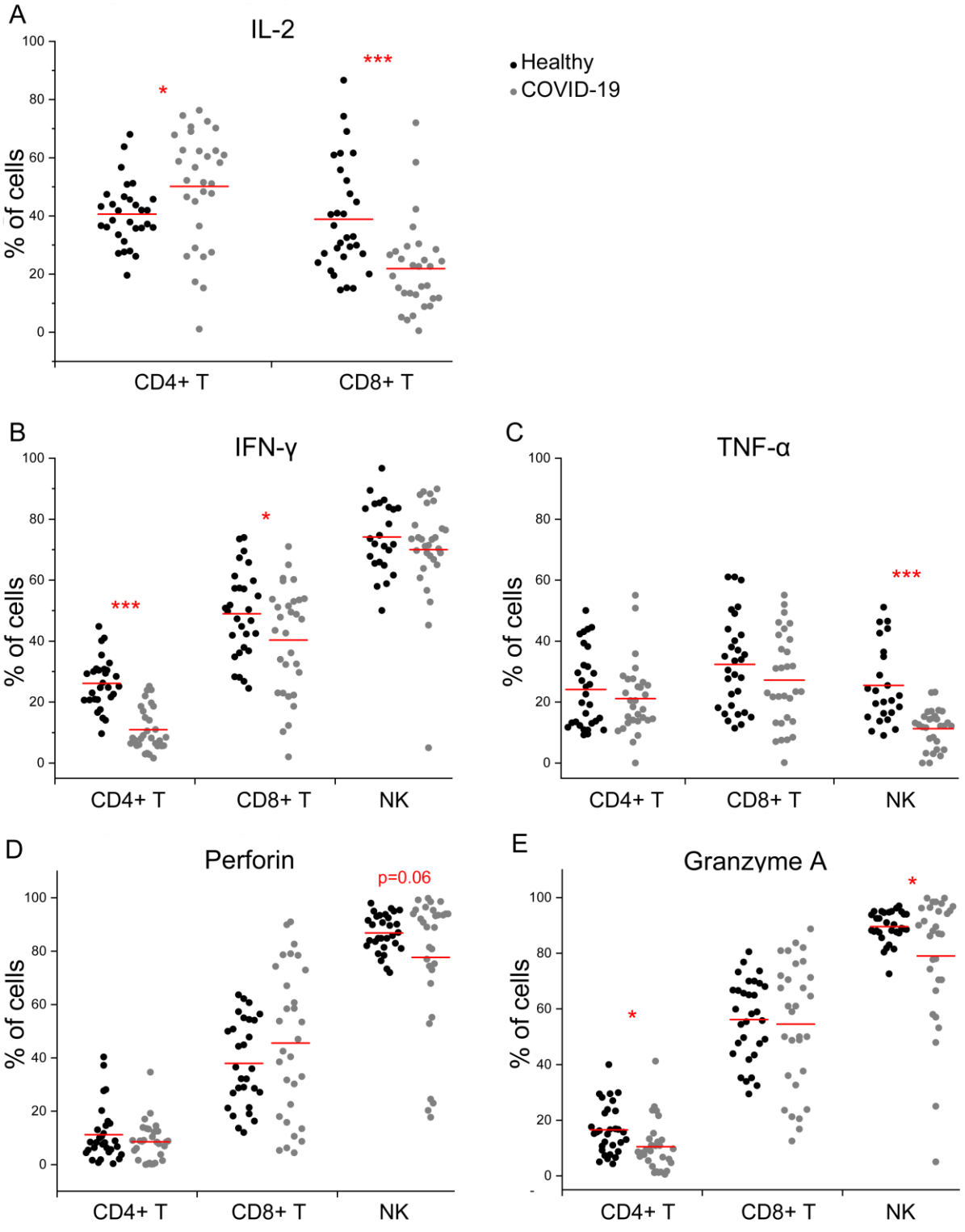

Figure 3. Functional characterization of CD4+ and CD8+ T and NK cells in COVID-19 patients

(A) Frequency of IL-2 secreting cells among CD4+ and CD8+ T cells following in vitro polyclonal stimulation in healthy donors (black dots) and COVID-19 patients (gray dots). Frequency of IFN-γ (B) and TNF-α (C) secreting cells among CD4+ and CD8+ T and NK cells

following in vitro polyclonal stimulation in healthy donors (black dots) and COVID-19 patients (gray dots). Frequency of Perforin (D) and Granzyme A (E) expressing cells among CD4+ and CD8+ T and NK cells in healthy donors (black dots) and COVID-19 patients (gray dots). Data have been obtained from 30 healthy controls and 30 COVID-19 patients. Red lines represent mean values for each population. *$p<0.05$; ***$p<0.001$ calculated with Student's T test.

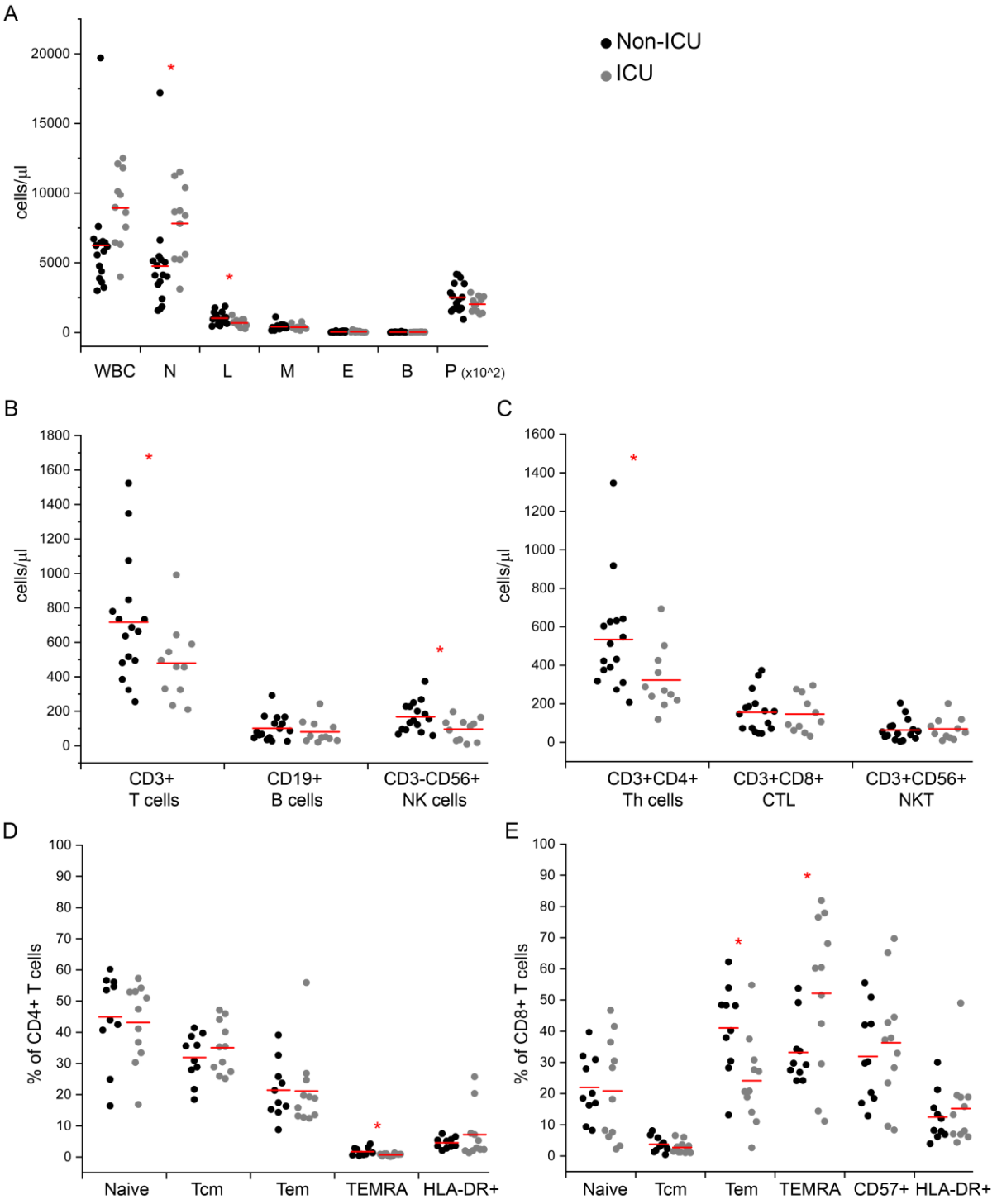

Figure 4. Absolute numbers of immune cell subsets in non-ICU versus ICU hospitalized COVID-19 patients

(A) Absolute numbers of total white blood cells (WBC), neutrophils (N), lymphocytes (L), monocytes (M), eosinophils (E), basophils (B), platelets (P) in non-ICU (black dots) and ICU (gray dots) COVID-19 patients. (B) Absolute numbers of CD3+ T cells, CD19+ B cells and

CD56+ NK cells in non-ICU (black dots) and ICU (gray dots) COVID-19 patients. (C) Absolute numbers of CD3+CD4+ T helper cells, CD3+CD8+ cytotoxic T cells (CTL), CD3+CD56+ NKT cells in healthy controls (black dots) and COVID-19 patients (gray dots). (D) Frequency of naïve (CD45RA+CCR7+), central memory (CD45RA-CCR7+), effector memory (CD45RA-CCR7-), TEMRA (CD45RA+CCR7-) and HLA-DR+ cells among CD4+ T cells in non-ICU (black dots) and ICU (gray dots) COVID-19 patients. (E) Frequency of naïve (CD45RA+CCR7+), central memory (CD45RA-CCR7+), effector memory (CD45RA-CCR7-), TEMRA (CD45RA+CCR7-), senescent (CD57+) and HLA-DR+ cells among CD8+ T cells in non-ICU (black dots) and ICU (gray dots) COVID-19 patients. Red lines represent mean values for each population. Data in A-C have been obtained from 16 non-ICU and 11 ICU COVID-19 patients. Data in D-E have been obtained from 10 non-ICU and 11 ICU COVID-19 patients. Red lines represent mean values for each population. *$p<0.05$ calculated with Student's T test.

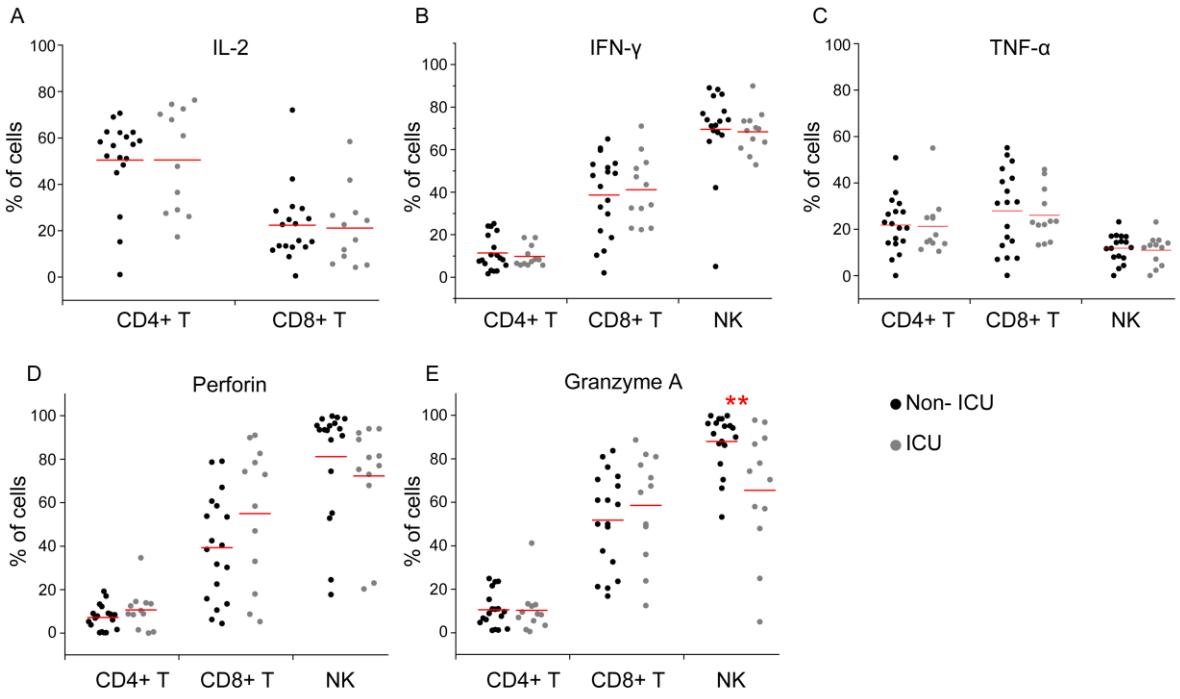

Figure 5. Immune cell functional characterization in non-ICU versus ICU hospitalized COVID-19 patients

(A) Frequency of IL-2-producing cells among CD4+ and CD8+ T cells following in vitro polyclonal stimulation in non-ICU (black dots) and ICU hospitalized patients (gray dots). Frequency of IFN-γ (B) and TNF-α (C) positive cells among CD4+ and CD8+ T and NK cells following in vitro polyclonal stimulation in non-ICU (black dots) and ICU hospitalized patients (gray dots). Frequency of Perforin (D) and Granzyme A (E) expressing cells among CD4+ and CD8+ T and NK cells in non-ICU (black dots) and ICU hospitalized patients (gray dots). Data have been obtained from 18 non-ICU and 12 ICU COVID-19 patients. **p<0.01 calculated with Student's T test.

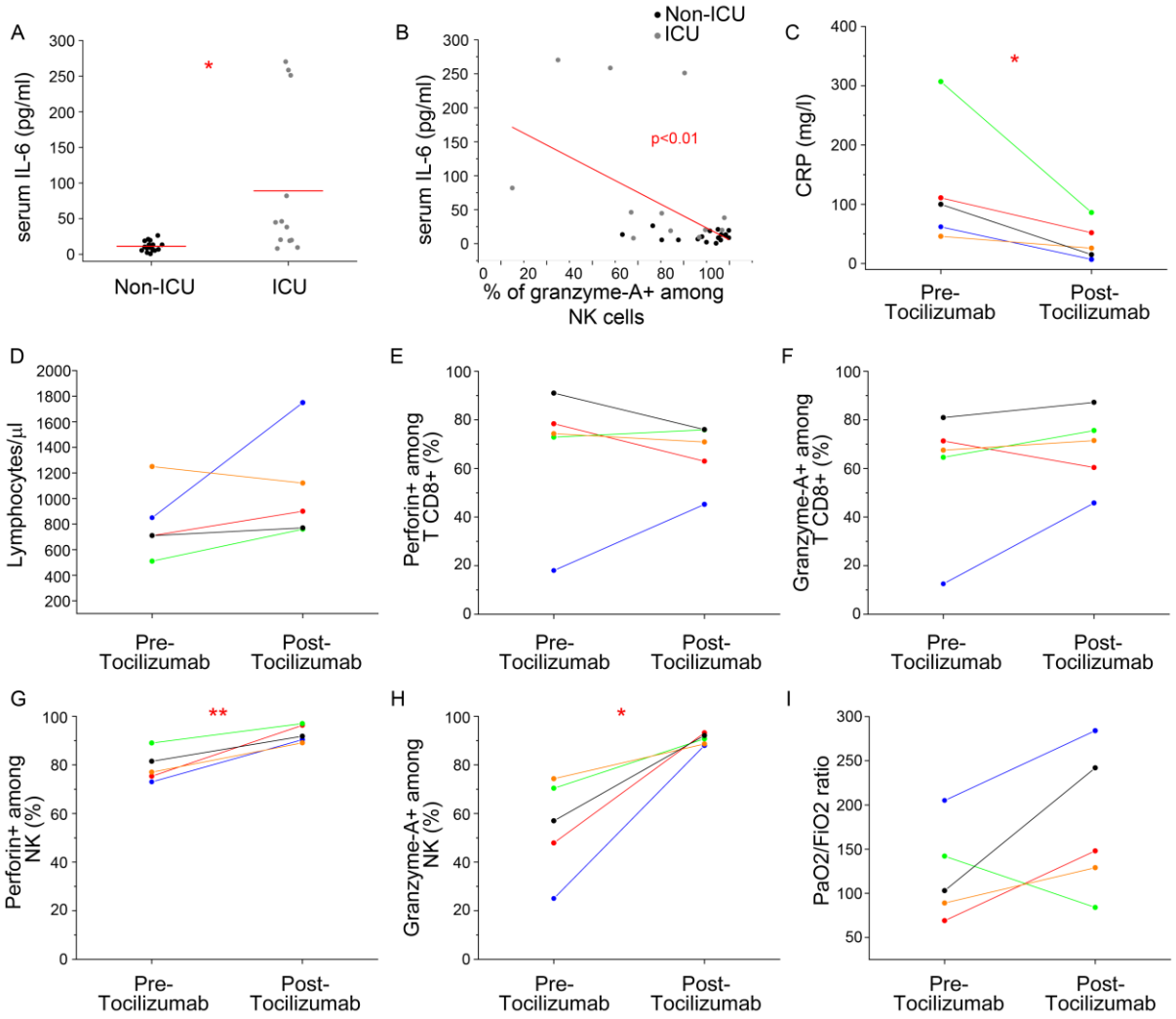

Figure 6. Biological effects of tocilizumab administration in COVID-19 patients

(A) IL-6 serum levels in non-ICU and ICU COVID-19 patients. Data represent mean ±SD. *p<0.05 calculated with Student's T test. (B) Correlation between serum IL-6 levels and percentage of Granzyme A+ cells among NK cells in non-ICU (black dots) and ICU (gray dots) COVID-19 patients, calculated with Pearson's correlation coefficiency. Red line represent the trend line. Data presented in panel A and B have been obtained from 30 COVID-19 patients. Evaluation of (C) serum CRP, (D) absolute lymphocyte counts (E) Perforin+ cells among CD8+ T cells, (F) Granzyme-A+ cells among CD8+ T cells, (G) Perforin+ cells among NK cells, (H) Granzyme-A+ cells among NK cells, (I) PaO2/FiO2 ratio in 5 selected ICU COVID-19 patients prior and after (72 hours) tocilizumab treatment. Each color line represents the same patient in all plots. *p<0.05; **p<0.01 calculated with Student's T test.

Supplementary items

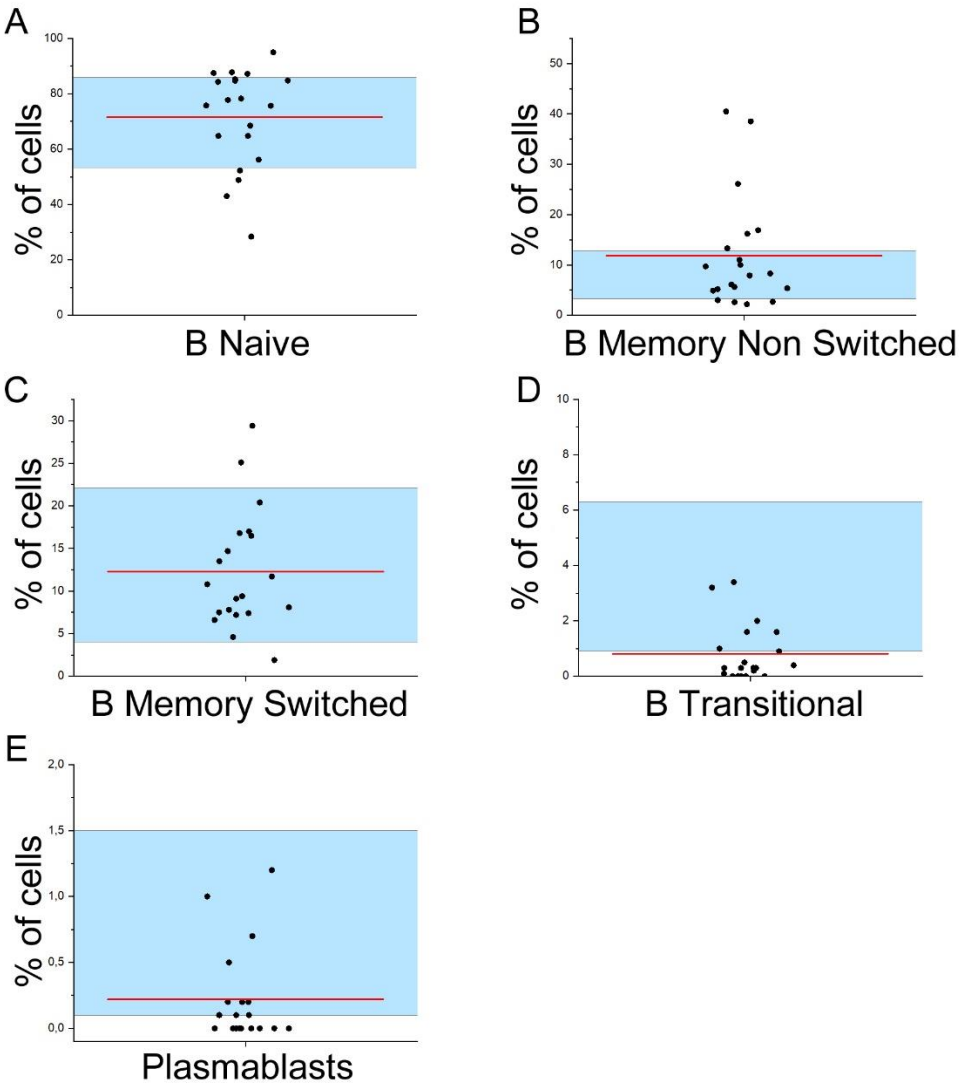

Figure S1. Frequency of B cell subsets in COVID-19 patients

Frequency of naïve (IgD+CD27-) (A), memory non switched (IgD+CD27+) (B), memory switched (IgD-CD27+) (C), transitional ($IgM^{high}CD38^{high}$) (D), plasmablasts ($CD27^{high}CD38^{high}$) (E) among CD19+CD20+ B cells in COVID-19 patients. The normality range is highlighted in light blue. Red lines represent mean values for each population. Data have been obtained from 20 COVID-19 patients.

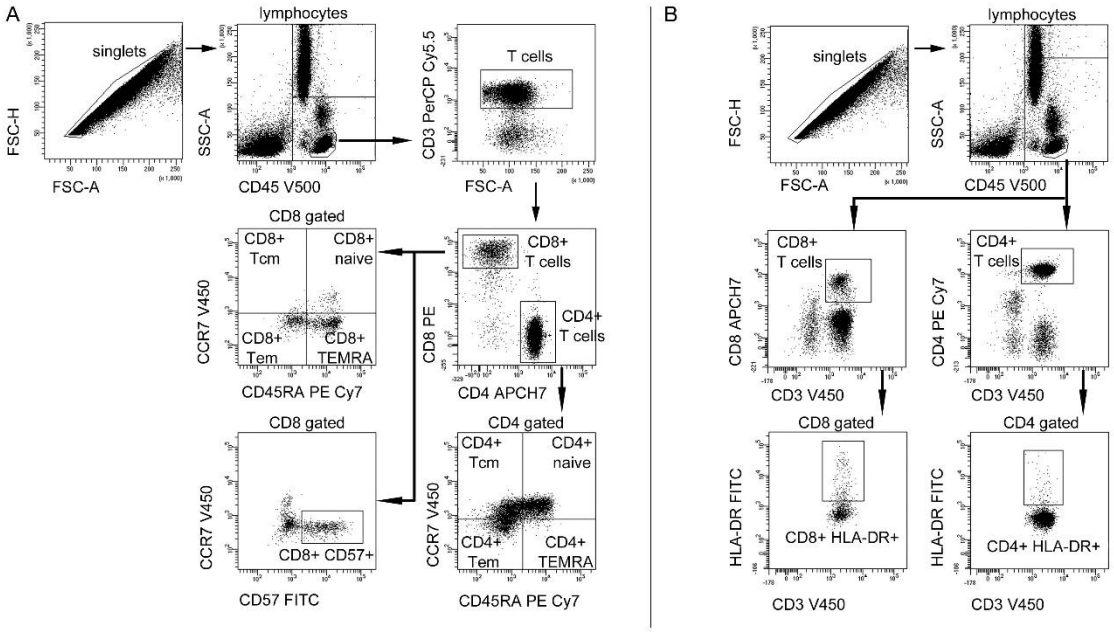

Figure S2. Gating strategy for the identification of CD4+ and CD8+ T cell subsets

In both the indicated panels (A, B) singlets were gated based on FSC-A and FSC-H parameters and then total lymphocytes were identified for CD45 positivity and low SSC-A. (A) T cells were identified as CD3+ cells and further divided in CD4+ and CD8+ subsets. CD4- and CD8-gated T cells were then analyzed for CCR7 and CD45RA expression thus identifying naïve (CD45RA+CCR7+), central memory (CD45RA-CCR7+), effector memory (CD45RA-CCR7-), TEMRA (CD45RA+CCR7-) cells. Senescent cells were finally identified on CD8+ T cells as CCR7- CD57+ cells. (B) Among total lymphocytes, CD3+CD4+ and CD3+CD8+ T cells were gated and evaluated for HLA-DR expression. These plots are representative of one COVID-19 patient.

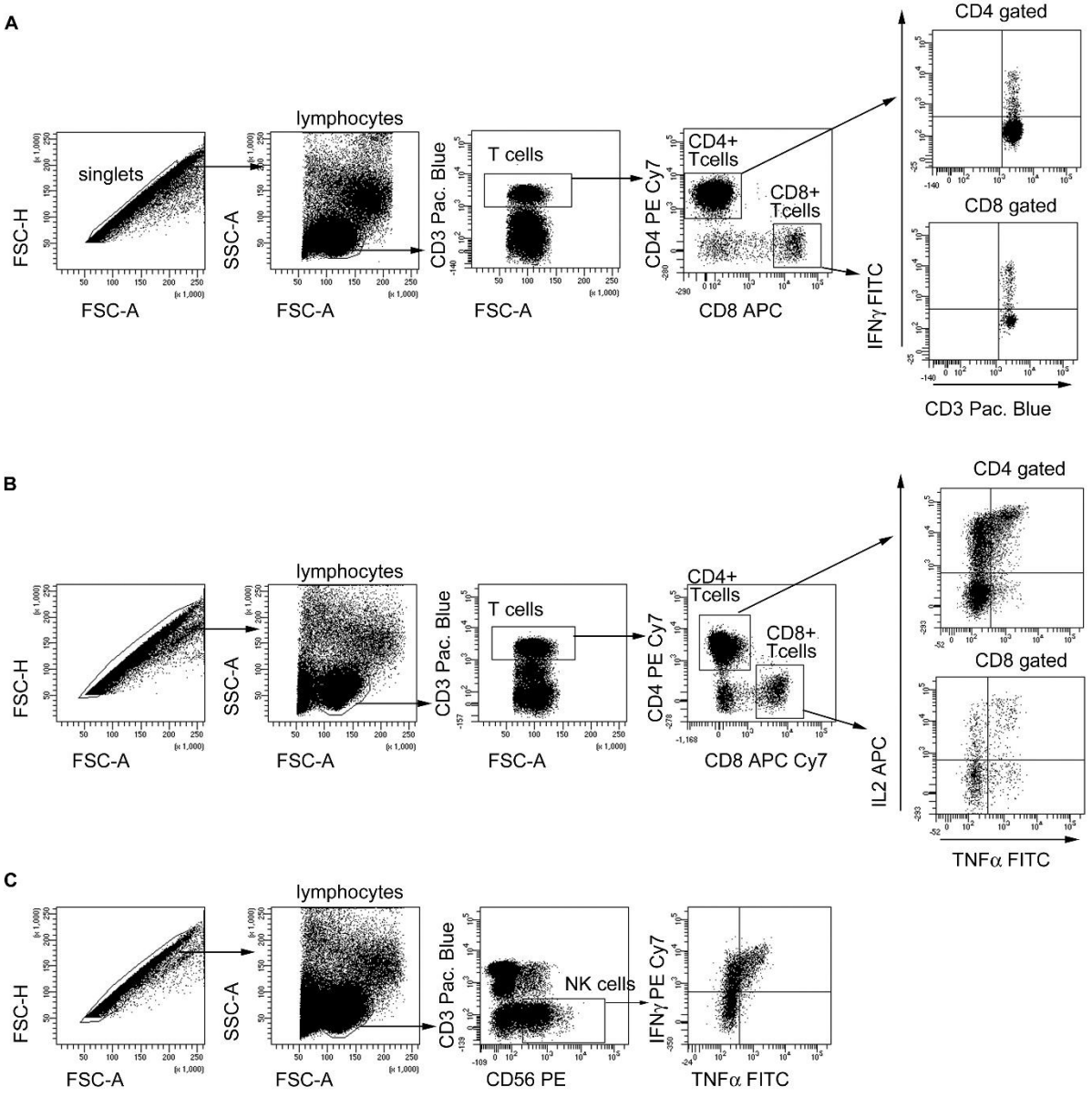

Figure S3. Gating strategy for the identification of cytokine-producing CD4+ and CD8+ T cells and NK cells

(A) Singlets were gated based on FSC-A and FSC-H parameters and then total lymphocytes were identified based on FSC-A and SSC-A parameters. T cells were gated as CD3+ and then further divided in CD4+ and CD8+. Finally, IFN-γ production was evaluated on these two T cell populations. (B) Singlets were gated based on FSC-A and FSC-H parameters and then total lymphocytes were identified based on FSC-A and SSC-A parameters. T cells were gated as CD3+ and then further divided in CD4+ and CD8+. Finally, TNF-α and IL-2 production were evaluated on these two T cell populations. (C) Singlets were gated based on FSC-A and

FSC-H parameters and then total lymphocytes were identified based on FSC-A and SSC-A parameters. NK cells were gated as CD3- CD56+. Finally, TNF-α and IFN-γ were evaluated. These plots are representative of one COVID-19 patient.

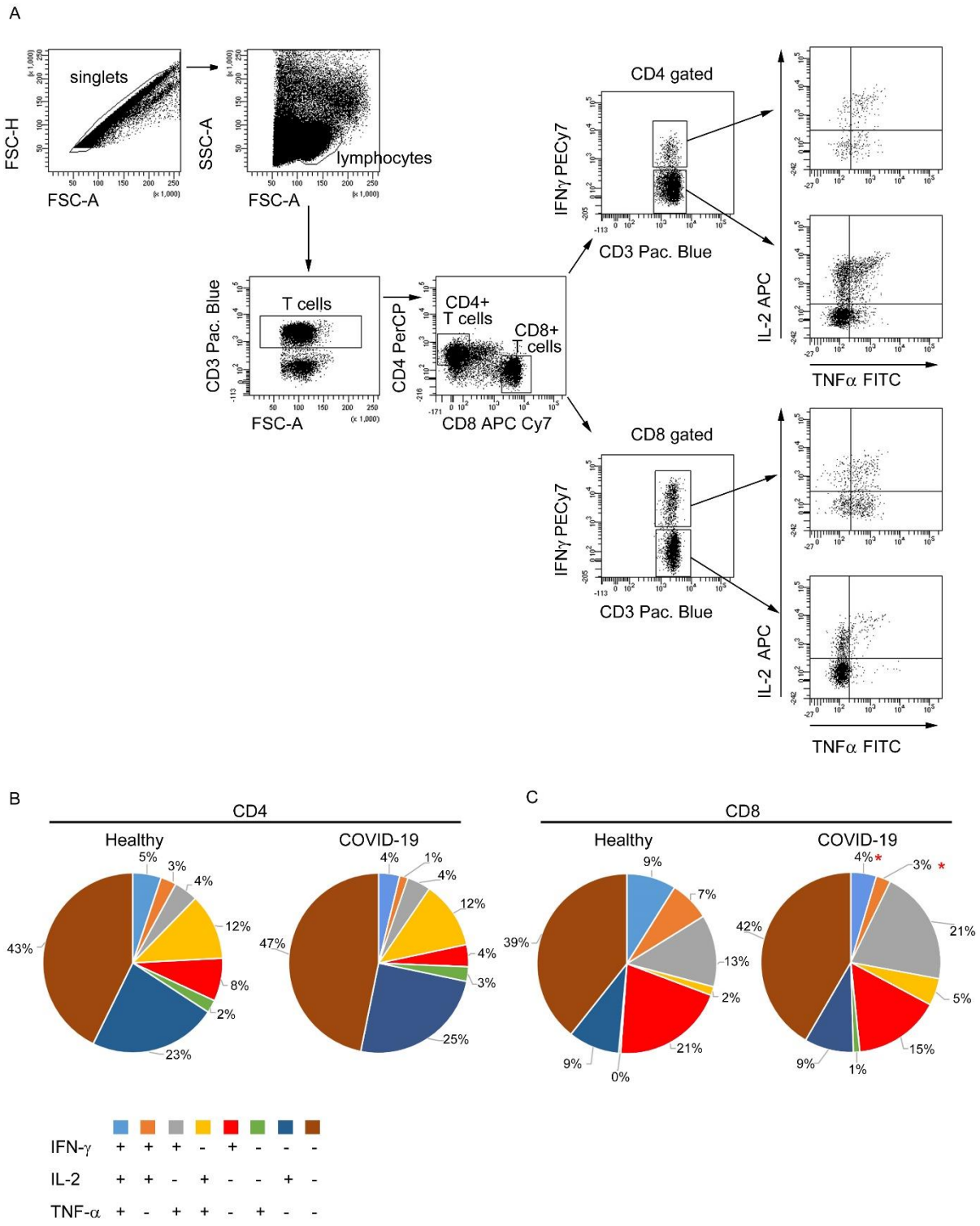

Figure S4. Characterization of T cell polyfunctionality in COVID-19 patients

(A) Gating strategy on a representative COVID-19 patient for the identification of polyfunctional CD4+ and CD8+ T cells. Singlets were gated based on FSC-A and FSC-H parameters and then total lymphocytes identified by physical parameters. T cells were

identified as CD3+ cells and further divided in CD4+ and CD8+ subsets. Among these two populations, we then identified both IFN-γ+ and IFN-γ- cells. Finally, we evaluated TNF-α and IL-2 production by both IFN-γ+ and IFN-γ- CD4+ and CD8+ T cells. Frequency of CD4 (B) or CD8 (C) T cells producing combinations of IFN-γ, IL-2, TNF-α in healthy individuals and COVID-19 patients. Pie charts represent percentages of total CD4+ or CD8+ T cells. Reported data are mean values obtained from 9 healthy individuals and 12 COVID-19 patients. *$p<0.05$ healthy versus COVID-19, calculated with Student's T test.

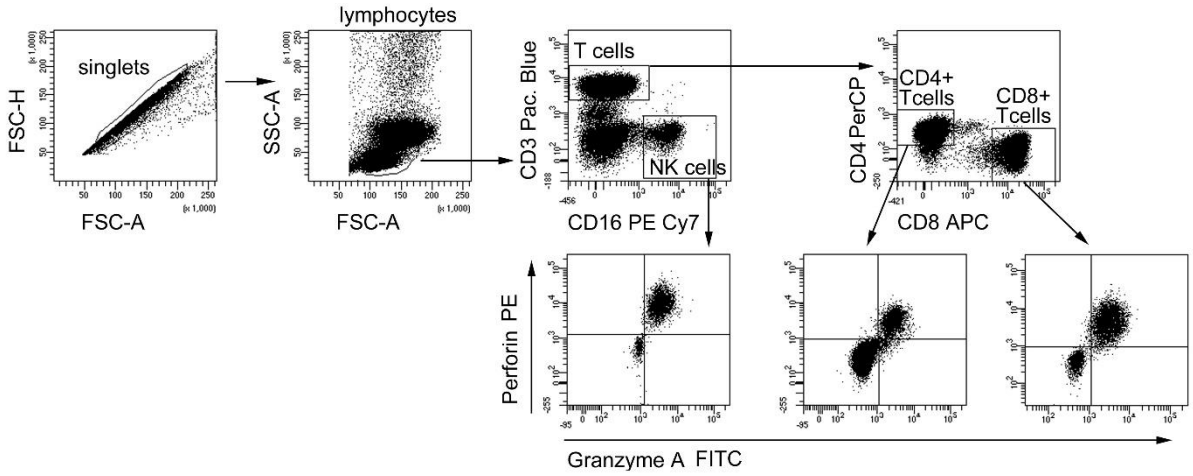

Figure S5. Gating strategy for the identification of cytotoxic molecules expression by CD4+ and CD8+ T and NK cells

Singlets were gated based on FSC-A and FSC-H parameters and then total lymphocytes identified based on physical parameters. T cells were then identified as CD3+ cells and further divided in CD4+ and CD8+ subsets. Among CD3- cells, we identified NK based on CD16 expression. Finally, we evaluated granzyme A and perforin expression on CD4+, CD8+ T lymphocytes and NK cells.

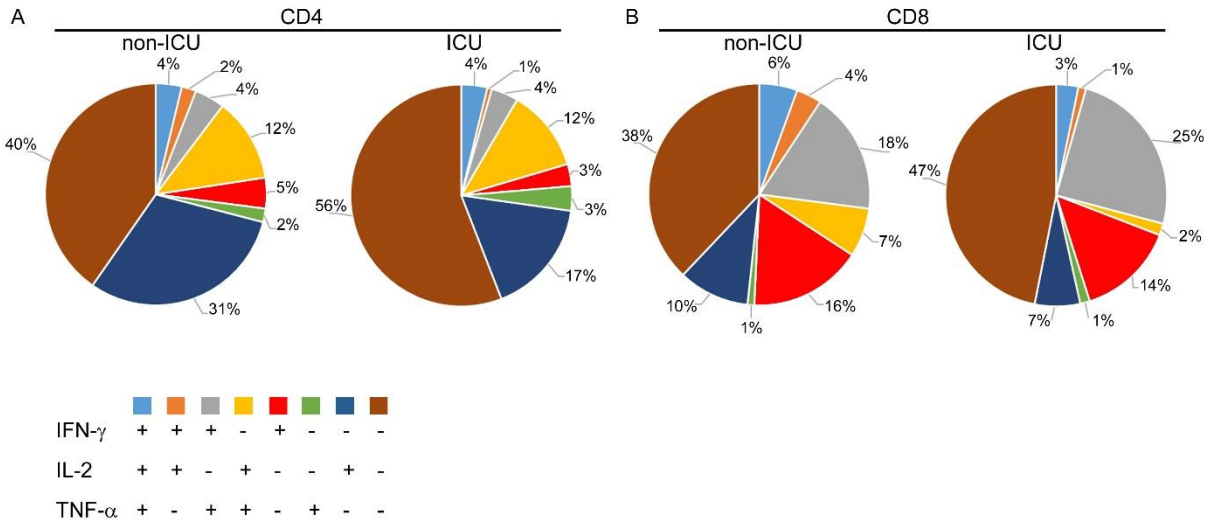

Figure S6. Characterization of T cell polyfunctionality in non-ICU and ICU COVID-19 patients

Frequency of CD4+ (A) or CD8+ (B) T cells producing combinations of IFN-γ, IL-2, TNF-α in non-ICU and ICU COVID-19 patients. Pie charts represent percentages of total CD4+ or CD8+ T cells. Reported data are mean values obtained from 7 non-ICU and 5 ICU COVID-19 patients.

Table S1: Clinical features of COVID-19 patients

A&S: general anaesthetics and sedatives; AF: atrial fibrillation; AI: autoimmune disease; ARDS: acute respiratory distress syndrome; BPH: benign prostatic hyperplasia; C: ceftriaxone; CBV: cerebrovascular disease; CKD: chronic kidney disease; COPD: chronic obstructive pulmonary disease; CT: computed tomography; CVD: cardiovascular disease; CXR: chest X-ray; D/C: darunavir/cobicistat; DBT: diabetes; DYS: dyslipidaemia; H: hypertension; HCQ: hydroxychloroquine; HRTC: high-resolution computed tomography; IV: invasive ventilation; K: malignant tumour; ICU: intensive care unit; P/T: piperacillin/tazobactam; LMWH: low-molecular-weight heparin; L/R: lopinavir/ritonavir; NC: nasal cannula; NIV: non-invasive ventilation; NRB: non-rebreather mask; OSAS: obstructive sleep apnoea syndrome; RIST: recent (<1 month) immunosuppressive therapy; RSP: recent (<1 month) surgical procedure; S: active smoker; SLSN: Senior-Løken syndrome; UCTD: undifferentiated connective tissue disease; US: thoracic ultrasound; VM: venturi mask

Patient	Gender	Age at onset	Days from clinical onset to analysis date	Symptoms/signs on analysis date	Most recent lung imaging findings	Comorbidities/Other states	Complications	Therapy on analysis date	Oxygen therapy on analysis date (FiO_2)	Mechanical ventilation during the course of the disease	Condition on analysis date (D=day from hospital admission)	Follow-up (d=day from analysis date)
1	F	71	8	Fever, dyspnoea, respiratory distress	Multiple bilateral patchy opacities (CXR)	H	ARDS	L/R, HCQ, C, P/T	VM (50%)	No	Hospitalized (D5)	Clinically recovered, discharged home (d7)
2	M	71	15	Diarrhea	Left lobar consolidation (CXR)	H	None	C	None	No	Hospitalized, clinically recovered (D5)	Discharged home (d7)
3	M	76	15	None	Multiple bilateral patchy opacities (CXR)	H, DBT, RSP (hernioplasty)	None	P/T, linezolid, azithromycin	VM (35%)	No	Hospitalized, clinically recovered (D2)	Discharged home (d7)
4	M	69	2	Fever, dyspnoea, respiratory distress	Multiple bilateral patchy opacities (CXR)	H, CVD, DBT, DYS	ARDS	D/C, HCQ	VM (50%)	Yes, IV	Hospitalized (D2)	Transferred in ICU on d2; in ICU until d19; clinically recovered, discharged home (d33)
5	M	64	5	Fever, dyspnoea, respiratory distress	Ground-glass opacities in the right superior lobe and left inferior lobe(CXR)	CVD, asthma	ARDS	L/R, HCQ, C, azithromycin, bisoprolol, ASA, clopidogrel, losartan	VM (40%)	Yes, IV	Hospitalized (D1), transferred in ICU on the same date	In ICU until d23; clinically recovered, discharged home (d36)
6	F	70	11	Fever, cough, myalgia	Bilateral basal interstitial thickening (CXR)	H, AI (rheumatoid arthritis)	None	D/C, HCQ	NC (28%)	No	Hospitalized (D2)	Clinically recovered, discharged home (d5)
7	M	52	13	None	Peribronchovascular interstitial thickening (CXR)	H, CVD, AF, OSAS	None	C, L/R, HCQ, LMWH	NC (24%)	No	Hospitalized, clinically recovered (D7)	Discharged home (d1)
8	F	63	10	Fever, cough	Multiple bilateral patchy opacities (CXR)	H	None	L/R, HCQ, C, azithromycin	NC (28%)	No	Hospitalized (D2)	Clinically recovered, discharged home (d4)
9	M	72	15	Sedated	Right basal consolidation and interstitial abnormalities (CXR)	CVD, AF, DBT, K (prostate), RSP (prostatectomy)	ARDS	Remdesivir, HCQ, A&S	IV (60%)	Yes, IV	ICU (D7)	Deceased (d28)
10	M	56	1	Fever	Left lobar consolidation (CXR)	Tetraplegia	None	L/R, HCQ, P/T	NC (28%)	No	Hospitalized (D3)	Clinically recovered, discharged home (d5)
11	F	36	5	Cough	Right basal consolidation and interstitial abnormalities (CXR)	Renal transplant in SLSN, RIST (tacrolimus)	None	C, low-dose methyl-prednisolone	None	No	Hospitalized (D5)	Clinically recovered, discharged home (d5)
12	M	84	6	Syncope, dyspnoea	Left pleural effusion, signs of pulmonary congestion (CXR)	H, CVD, CBV, DBT	ARDS	D/C, C, azithromycin, insulin	NC (24%)	No	Hospitalized (D5)	Deceased (d7)
13	M	78	23	Fever, cough	Multiple bilateral patchy opacities (CXR)	None	None	L/R, P/T	None	No	Hospitalized, clinically recovered (D9)	Discharged home (d2)

14	F	62	6	Fever	Ground-glass opacities in the left superior lobe and right superior lobe (HRCT)	None	None	D/C, HCQ	None	No	Hospitalized, clinically recovered (D1)	Discharged home (d1)
15	M	80	6	Sedated	Multiple bilateral consolidations and groun-glass opacities, pleural effusion, hilar lymphadenopathy (HRTC)	H, AF, OSAS, BPH	ARDS, acute kidney injury	Meropenem, linezolid, azithromycin, norepinephrine, bisoprolol, amiodarone, insulin, acetylcysteine, LMWH, A&S	IV (30%)	Yes, IV	ICU (D1)	In ICU until d40; hospitalized (d44)
16	M	65	6	Fever, respiratory distress, sedated	Multiple bilateral consolidations (CXR)	None	ARDS	D/C, HCQ, meropenem, linezolid, azithromycin, norepinephrine, LMWH, A&S	IV (80%)	Yes, IV	ICU (D1)	In ICU until d25; hospitalized (d44)
17	M	45	8	Fever, cough	Ground-glass opacities in the left lung, interstitial abnormalities (CXR)	None	ARDS	D/C, HCQ, P/T, azithromycin	NRB 80%	No	ICU (D0)	Clinically recovered, discharged home (d7)
18	F	60	unknown	Cough	Right superior lobe consolidation; right lower lobe opacity (CXR)	H	None	D/C, HCQ	None	No	Clinically recovered (D4)	Discharged home (d2)
19	F	70	9	Fever, cough, myalgia	Multiple bilateral ground-glass opacities (CT)	K, DYS	ARDS	D/C, HCQ	NC (36%)	No	Hospitalized (D3)	Clinically recovered, discharged home (d15)
20	M	74	9	Fever, cough	Left superior lobe consolidations (CXR)	H	Acute respiratory failure (w/o ARDS)	L/R, HCQ	NC (28%)	No	Hospitalized (D2)	Clinically recovered, discharged home (d10)
21	F	73	11	None	Left lung consolidations (CXR)	None	None	L/R, HCQ	None	No	Clinically recovered (D5)	Discharged home (d0)
22	M	72	7	Fever	Multiple bilateral patchy opacities (CXR)	CVD	ARDS	L/R, HCQ, general anesthetics and sedatives	IV (50%)	Yes, IV	Hospitalized (D2), transferred in ICU on the same date	ICU (d43)
23	M	79	unknown	Syncope, subcutaneous emphysema	Right pleural effusion, no consolidations (CXR)	K (lung), RSP (right middle lung lobectomy), H, DBT, DYS, COPD, S	Acute respiratory failure (w/o ARDS)	L/R, HCQ, ASA, bisoprolol, losartan, LMWH, amoxicillin/clavulanic acid	NC (36-44%)	No	Hospitalized (D14)	Clinically recovered, discharged home (d14)
24	F	40	8	Fever, cough	Multiple bilateral consolidations (US)	None / 25 weeks pregnant	ARDS	L/R, HCQ, ertapenem, azithromycin	VM (60%)	Yes, NIV	Hospitalized (D2)	In ICU until d7; clinically recovered, discharged home (d18)
25	M	46	11	Fever	Bilateral interstitial pneumonia (CXR)	AI (psoriatic arthritis), RIST (ustekinumab)	ARDS	L/R, HCQ	NC (28-36%)	No	Hospitalized (D3)	Clinically recovered, discharged home (d5)
26	F	48	8	Cough	Righ inferior lobe consolidation (US)	AI (thyroiditis, UCTD) / 25 weeks pregnant	None	L/R, HCQ	None	No	Hospitalized (D1)	Clinically recovered, discharged home (d10)
27	M	70	9	Respiratory distress	Multiple bilateral patchy opacities (CXR)	H, S	ARDS	L/R, HCQ	NIV (100%) then IV (80%)	Yes, IV	ICU (D2)	In ICU until d12 when transferred to another hospital

28	F	85	9	Dyspnoea, cough, respiratory distress	Bilateral pleural effusion, peripheral patchy opacities, pulmonary congestion (CXR)	H, CVD, AF, CKD, DBT, COPD, S	ARDS, acute on chronic cardiac failure	D/C, HCQ, C, azithromycin, warfarin, furosemide, losartan, acetylcysteine, medium-dose methylprednisolone	NIV (80%)	Yes, NIV	ICU (D6)	Deceased (d27)
29	F	78	17	Respiratory distress	Multiple bilateral consolidations (CXR)	H	ARDS	D/C, HCQ, ramipril, azithromycin, amlodipine, LMWH	NRB (80%) then NIV (80%)	Yes, NIV	ICU (D2)	In ICU until d25; hospitalized (d40)
30	M	70	5	Fever, cough, respiratory distress	Bilateral diffuse interstitial abnormalities, no consolidations (CXR)	H, DYS	ARDS	HCQ, P/T, azithromycin, furosemide, acetylcysteine, LMWH, A&S	NIV (100%)	Yes, NIV	ICU (D1)	Deceased (d9)

Table S2: Laboratory tests in COVID-19 patients on analysis date

Patient	Hematocrit (%) (reference range 42-52)	Hb (g/dL) (reference range 14-18)	MCV (fL) (reference range 81-94)	RBC ($x10^{12}$/L) (reference range 4.2-5.4)	WBC ($x10^6$/L) (reference range 4000-10000)	Neutrophils ($x10^6$/L) (reference range 1500-7500)	Lymphocytes ($x10^6$/L) (reference range 500-5000)	Neutrophils to lymphocytes ratio	Monocytes ($x10^6$/L) (reference range 30-1200)	Eosinophils ($x10^6$/L) (reference range 0-700)	Basophils ($x10^6$/L) (reference range 0-200)	Platelets ($x10^6$/L) (reference range 140000-400000)	Creatinine (mg/dL) (reference range 0.7-1.2)	Alanino-aminotransferase (U/L) (reference range 10-50)	Gamma-GT (U/L) (reference range 10-71)	Creatine kinase (U/L) (reference range 39-308)	C-reactive protein (mg/L) (normal value <5)	Fibrinogen (mg/dL) (reference range 200-400)	Lactate dehydrogenase (U/L) (reference range 135-225)	Ferritin (ng/mL) (reference range 8-252)	D-dimer (ng/mL) (normal value <500)	IL-6 (pg/mL) (reference range 0-10)
1	38.9	12,6	94	4.14	4390	3640	480	7.6	240	10	20	230000	0.53	33	-	-	201	-	438	-	-	12.4
2	38.9	12.6	91.5	4.16	6440	5220	720	7.3	460	20	20	209000	0.97	24	-	-	55	-	224	-	-	13.3
3	37.7	12.3	88.7	4.25	7610	6620	700	9.5	280	0	10	187000	0.98	31	-	281	108	639	283	-	-	21
4	33.9	10.9	91.1	3.72	3990	3110	520	6.0	300	40	20	151000	-	-	-	-	-	291	398	-	-	20.3
5	40.7	13.6	91.3	4.46	12500	11500	520	22.1	370	90	20	263000	0.84	32	-	72	140	814	433	-	-	38
6	41.4	13.7	95	4.36	6530	5450	560	11.4	480	10	20	172000	0.75	11	-	42	44	510	210	-	-	13.3
7	46.9	15.1	88.5	5.30	6240	4120	1460	2.8	560	80	20	414000	1.08	39	-	-	<5	-	162	-	-	8.6
8	38.6	12.8	92.1	4.19	6440	4800	1070	4.5	410	120	40	393000	0.67	41	-	-	-	-	-	-	-	19.6
9	28.8	9.1	94.4	3.05	4350	-	-	-	-	-	-	-	2.14	-	-	-	432	704	271	-	-	251
10	37.7	12.4	87.1	4.33	4760	3440	830	4.1	400	10	80	159000	0.37	61	-	29	58	383	198	-	-	9.4
11	42.1	13.3	95.7	4.40	19700	17200	1300	13.2	1120	40	40	352000	2.19	10	-	19	70	-	186	453	-	10.3
12	-	-	-	-	-	-	-	-	-	-	-	-	0.86	22	-	467	-	-	271	-	-	18.7
13	38.6	12.1	89.4	4.32	6700	5030	990	5.1	540	100	40	418000	1.4	20	-	-	28	-	-	-	-	0.48
14	40.2	13.2	92.8	4.33	3600	1670	1770	0.9	150	0	10	167000	0.63	42	-	67	11	442	267	-	-	6.8
15	37.6	12.2	91.5	4.13	11800	11230	310	36.2	150	80	30	193000	1.95	94	52	-	92	563	531	-	-	81.9
16	40.4	13.3	93.3	4.33	6310	5220	850	6.1	210	10	20	200000	1.23	57	195	-	62	432	717	-	1071	270.2
17	38.8	12.7	89	4.36	12100	10390	910	11.4	750	10	40	232000	0.64	43	35	-	64	531	279	-	265	9.4
18	38.6	12.9	90.6	4.26	3870	1570	1870	0.8	310	100	20	252000	0.59	18	-	78	23	507	228	-	-	5.3
19	40.2	12.8	87.4	4.6	5830	4090	1450	2.8	290	0	0	260000	0.85	35	-	64	47	-	234	-	-	8.6
20	44	14.5	94	4.68	5560	4010	1070	3.7	470	0	10	174000	1.19	14	-	104	59	483	247	430	558	26.4
21	36.8	11.6	90	4.09	3210	1840	940	2	360	40	30	349000	1.08	47	-	67	8	398	206	531	294	5.5
22	38.6	12.9	89.6	4.04	6430	5270	710	7.4	290	140	20	129000	0.94	24	20	290	100	406	369	779	959	46.1
23	26.7	8.6	96.7	2.76	11500	-	-	-	-	-	-	285000	0.7	-	38	-	32	246	238	-	1813	2.3
24	28.0	8.8	63.9	4.38	10100	8740	920	9.5	390	10	40	226000	0.51	96	24	-	-	-	-	-	-	8.05
25	40.8	14	86.4	4.72	6170	5120	620	8.3	310	110	10	152000	0.89	52	-	-	71	-	341	1118	1204	13.4
26	33.8	11.1	94.7	3.57	2990	2400	430	5.6	150	10	0	93000	0.71	50	-	18	29	552	165	51	889	5.5
27	43.1	14.9	88.3	4.88	9880	8660	710	12.2	320	180	10	152000	1.12	28	108	-	111	639	483	2394	727	258.5
28	28.6	8.4	88.5	3.23	8970	8390	260	32.3	310	0	10	257000	2.19	-	39	-	151	-	606	936	1176	19.9
29	42	13.9	97	4.33	7570	5600	1250	4.5	680	30	10	287000	0.81	38	100	-	46	510	431	811	921	18.9
30	41	13.3	91.3	4.49	8620	7810	510	15.3	280	10	20	138000	0.88	36	48	-	307	846	537	1058	28426	44.7

Table S3: Arterial blood gas test in COVID-19 patients on analysis date

A. Estimated normal paO_2 (mmHg) equals to (100) – (0.3) x (age in years)
B. Alveolar-arterial O_2 gradient (mmHg) equals to [(FiO2) x (Atmospheric Pressure - H_2O Pressure) – ($PaCO_2$/0.8)] – (PaO_2)
C. Expected Alveolar-arterial O_2 gradient for age (mmHg) equals to [(age in years)/4] + 4

Patient	pH (reference range 7.35-7.45)	FiO2 (%)	PaO_2 (mmHg)	$PaCO_2$ (mmHg)	SaO_2 (%) (reference range 95-99)	HCO_3^- (mmol/L) (reference range 21-28)	Estimated normal PaO_2 (mmHg)[A]	PaO_2/FiO_2 ratio	SaO_2/FiO_2 ratio	Alveolar-arterial O_2 gradient (mmHg)[B]	Expected Alveolar-arterial O_2 gradient for age (mmHg)[C]
1	7.49	50	71.4	30.5	96.4	25	78.7	143	193	247	22
2	7.45	21	81.1	36.8	97.3	26	78.7	386	463	22.6	22
3	7.41	35	84.2	37.9	97.6	24	77.2	241	279	118	23
4	7.43	50	110	22.1	99.2	23	79.3	220	198	218.9	21
5	7.48	28	58.9	28.6	94	23	80.8	210	336	105	20
6	7.46	21	60.9	34	93.8	25	79.0	290	447	46.3	22
7	7.41	21	84.2	37.9	97.6	24	84.4	401	465	18.2	17
8	7.53	28	70.3	28.7	96.3	24	81.1	251	344	93.5	20
9	7.38	60	82	53	96.5	31	78.4	137	161	279.6	22
10	7.43	28	75.1	32.2	95.6	22	83.2	268	341	84.3	18
11	7.43	21	88.2	26.6	97.8	20	89.2	420	466	28.3	13
12	7.51	24	64.5	27.8	94	22	74.8	269	392	71.9	25
13	7.48	21	71.1	33	96	25	76.6	339	457	37.4	24
14	7.47	21	73.3	33	95	25	81.4	349	452	34.8	20
15	7.46	30	123	40.5	98.6	28	76.0	410	329	40.3	24
16	7.46	80	164	44	98	30	80.5	205	123	351.4	20
17	7.44	80	134	35	98	25	86.5	168	123	392.7	15
18	7.47	21	74.4	37.3	96.6	28	82.0	354	460	28.7	19
19	7.47	36	88.5	40.7	95	30	79.0	246	264	117.3	22
20	7.48	28	76.7	32.5	96	26	77.8	274	343	82.3	23
21	7.49	21	69.7	32.5	96	26	78.1	332	457	39.4	22
22	7.44	50	51.7	31.7	87.8	23	78.4	103	176	265.2	22
23	7.45	44	142	41	99.9	28	76.3	323	227	120.5	24
24	7.46	60	70	35.2	95.8	25	88	117	160	313.8	14
25	7.44	36	132	39.1	99.5	27	86.2	367	276	75.8	15.5
26	7.46	21	84.7	31.7	-	22.7	85.6	403	-	25.4	16
27	7.43	100	69	36.8	95	24	79	69	95	598	21.5
28	7.40	80	147	43	99.4	26	74.5	184	124	369.7	25.25
29	7.44	80	71	38	94.7	26	76.6	89	118	451.9	23.5
30	7.46	100	142	34.4	99	-	79	142	99	528	21.5

Table S4. Demographic characteristics of control subjects

Control	Age	Gender
1	39	M
2	50	F
3	53	M
4	56	M
5	57	M
6	58	F
7	59	F
8	59	M
9	60	M
10	60	F
11	61	F
12	62	M
13	62	F
14	62	M
15	63	F
16	64	M
17	64	M
18	64	M
19	64	M
20	66	F
21	66	F
22	68	F
23	69	F
24	70	M
25	75	F
26	76	F
27	77	F
28	77	M
29	79	M
30	84	F

Table S5. List of all fluorochrome mAbs used for flow cytometric analysis

Marker	Clone	Flurochrome	Company
CCR7	150503	Horizon™ V450	BDBioscience
CD127	HIL-7R-M21	Horizon™ V450	BDBioscience
CD16	3G8	PE-Cy™7 PerCP-cy5.5	BDBioscience
CD19	SJ25C1	PerCP-cy5.5 APC	BDBioscience
CD20	L27	APC-H7	BDBioscience
CD21	B-ly4	Horizon™ V450	BDBioscience
CD25	2A3	PE-Cy™7	BDBioscience
CD27	L128	APC	BDBioscience
CD3	UCHT1	Pacific Blue™ Horizon™ V450	BDBioscience
CD3	SK7	PerCP-cy5.5	BDBioscience
CD38	HB-7	PE-Cy™7	BDBioscience
CD4	SK3	PE-Cy™7 PerCP APC-Cy™7 APC-H7	BDBioscience
CD45	2D1	Horizon™ V500	BDBioscience
CD45RA	L48	PE-Cy™7	BDBioscience
CD56	MY31	PE	BDBioscience
CD56	NCAM16.2	PE	BDBioscience
CD57	HNK-1	FITC	BDBioscience
CD8	SK1	PE APC-Cy™7 APC APC-H7	BDBioscience
CXCR5	51505	PE	R&DSystems
Granzyme A	CB9	FITC	BDBioscience
HLA-DR	L243	FITC	BDBioscience
IFN-γ	B27	PE-Cy™7	BDBioscience
IFN-γ	25723.11	FITC	BDBioscience
IgD	IA6-2	PE	BDBioscience
IgM	G20-127	FITC	BDBioscience
IL-2	MQ1-17H12	APC	BDBioscience
Perforin	delta G9	PE	BDBioscience
TCRa/b	WT31	FITC	BDBioscience
TCRg/d	11F2	PE	BDBioscience
TNF-α	6401.1111	FITC	BDBioscience